

# Efficient Encoding of Matrix Product States into Quantum Circuits of One- and Two-Qubit Gates

Shi-Ju Ran<sup>1,\*</sup>

<sup>1</sup>*Department of Physics, Capital Normal University, Beijing 100048, China*

(Dated: September 25, 2022)

Matrix product state (MPS) belongs to the most important mathematical models in, for example, condensed matter physics and quantum information sciences. However, to realize an  $N$ -qubit MPS with large  $N$  and large entanglement on a quantum platform is extremely challenging, since it requires high-level qudits or multi-body gates of two-level qubits to carry the entanglement. In this work, an efficient method that accurately encodes a given MPS into a quantum circuit with only one- and two-qubit gates is proposed. The idea is to construct the unitary matrix product operators that optimally disentangle the MPS to a product state. These matrix product operators form the quantum circuit that evolves a product state to the targeted MPS with a high fidelity. Our benchmark on the ground-state MPS's of the strongly-correlated spin models show that the constructed quantum circuits can encode the MPS's with much fewer qubits than the sizes of the MPS's themselves. This method paves a feasible and efficient path to realizing quantum many-body states and other MPS-based models as quantum circuits on the near-term quantum platforms.

Matrix product state (MPS) is one of most successful mathematical tools in the contemporary physics. In condensed matter physics, MPS is the state ansatz behind the famous density matrix renormalization group (DMRG) algorithm [1, 2] and many of its variants [3–7]. MPS can efficiently describe the ground states and (purified) thermal states of one-dimensional (1D) gapped systems [8–12]. It has also been widely and successfully applied to other areas including statistic physics [13], non-equilibrium quantum physics [9, 14–17], field theories [18–23], machine learning [24–28], and so on.

In particular, MPS is an important model in quantum information and computation (see, e.g., [29–32]). It can represent a large class of states, including GHZ [33] and AKLT states [34, 35], which can implement non-trivial quantum computational tasks [36, 37]. However, the realization of MPS on quantum hardware is strictly limited. This is partially due to the fact that current techniques only permit short coherent time and small numbers of computing qubits. Solid progresses are reported in this direction recently, for instance, the realization of the GHZ state up to twenty qubits in a (relatively) long coherent time [38].

However, MPS is hindered by another essential difficulty. There are two kinds of degrees of freedom in MPS, which are physical degrees of freedom corresponding to the Hilbert space in which the physical system is defined, and the virtual degrees that carry the entanglement of the MPS. In general, the dimension of the virtual degrees of freedom (denoted as  $\chi$ ) is much larger than the physical dimension (denoted as  $d$ ). To realize an MPS in a quantum platform, one intuitively needs to realize  $\chi$ -level qudits as the virtual degrees of freedom. This becomes almost impossible considering we usually take  $\chi \sim O(10^2)$  or even larger.

Recently, an inspiring method named as qubit-efficient scheme was proposed by Huggins *et al* [27], where the  $\chi$ -level qudits in the circuits of MPS's are equivalently replaced by several two-level qubits. Since such a scheme contains multiple-qubit gates, one must further compile the multiple-qubit gates to one- and two-qubit gates to implement on the realistic quantum hardware [39, 40]. The MPS should be in

a form similar to, for instance, the state ansatz for the variational quantum eigensolvers [41]. However, compiling an MPS of large  $\chi$  is extremely inefficient, since the depth of the circuit generally scales polynomially with  $\chi$  [42]. Therefore, efficient encoding algorithms for MPS's are strongly desired.

In this work, we propose an algorithm that efficiently and accurately encodes a given MPS with  $d = 2$  and  $\chi \gg d$  into a quantum circuit consisting of only one- and two-qubit gates. The idea is to construct the unitary matrix product operators [43], dubbed as matrix product disentanglers (MPD's), that disentangle the targeted MPS. These MPD's form a multi-layer quantum circuit, which evolves a product state into the MPS with a high fidelity.

We testify our encoding algorithm on the MPS's that approximate the ground states of the 1D strongly-correlated spin systems. Since these MPS's possess large entanglement, it is obviously difficult to realize them on quantum circuits by the existing methods. We show that high fidelity between the MPS's and the evolved states by quantum circuits can be reached with only  $O(10)$  layers of MPD's. By incorporating with the qubit-efficient scheme [27], our method efficiently encodes the MPS's into a quantum circuit of less than 10 qubits, which is much less than the size of the MPS's themselves.

*Matrix product state and orthogonal form: preliminaries.*— An MPS [left part of Fig. 1 (a)] consisting of  $N$  sites (qubits or qudits) can be written as

$$|\Psi\rangle = \sum_{a_1 \cdots a_{N-1}} \sum_{s_1 \cdots s_N} A_{s_1, a_1}^{[1]} A_{s_2, a_1 a_2}^{[2]} \cdots A_{s_N, a_{N-1}}^{[N]} \prod_{n=1}^N |s_n\rangle. \quad (1)$$

The indexes  $\{s_n = 0, \dots, d-1\}$  represent the degrees of freedom of the physical sites, with  $d$  the number of the levers of each site.  $\{a_n\}$  (called virtual indexes) label the virtual degrees of freedom that carry the entanglement of the MPS. Normally in an MPS-based algorithm, we bound the virtual dimensions  $\dim(a_n) \leq \chi$  to control the computational cost (see for instance [1, 2, 11]), with  $\chi$  called the dimension cut-off.

Generally speaking, one needs to take  $\chi \gg d$  to sufficiently capture the entanglement. Take the MPS representing a one-dimensional (1D) critical state or conformal field theory as an example. One should take  $\chi \sim N^\alpha$ , where the exponent  $\alpha (\simeq 1)$  is determined by the central charge as well as the scaling laws of correlation length and entanglement entropy [44, 45].

An MPS can be transformed into different orthogonal forms. Let us focus on the left-orthogonal form that will be used later in this paper. The first tensor satisfies the normalization condition, and the rest satisfy the left-orthogonal conditions, i.e.,

$$|A^{[1]}| = \sum_{s_1 a_1} A_{s_1, a_1}^{[1]} A_{s_1, a_1}^{[1]*} = 1, \quad (2)$$

$$\sum_{s_n a_n} A_{s_n, a_{n-1} a_n}^{[n]} A_{s_n, a'_{n-1} a_n}^{[n]*} = I_{a_{n-1} a'_{n-1}} (1 < n < N), \quad (3)$$

$$\sum_{s_N} A_{s_N, a_{N-1}}^{[N]} A_{s_N, a'_{N-1}}^{[N]*} = I_{a_{N-1} a'_{N-1}}, \quad (4)$$

with  $I$  the identity. The orthogonal conditions in fact determine the directions of the renormalization-group flows in the Hilbert space [46].

*Encoding matrix product state into single-layer quantum circuit.*— Let us temporarily assume that the physical dimension of the MPS equals to the dimension cut-off, i.e.,  $d = \chi$ . Now we show that such an MPS can be exactly encoded into a quantum circuit consisting of only one- and two-body gates on the  $d$ -level qudits. For the rest of paper, we take  $d = 2$  without losing generality. Then a  $d$ -level qudit will be directly called a qubit. Note most of the arguments can be readily generalized to the cases of  $d > 2$ .

To the aim of encoding, we define an unitary matrix product operator  $\hat{U}$  that disentangles the MPS  $|\psi\rangle$  into a product state, i.e.,

$$\hat{U}|\psi\rangle = \prod_{n=1}^N |0\rangle_n \stackrel{\text{def}}{=} |0\rangle. \quad (5)$$

We dub such a matrix product operator as matrix product disentangler (MPD). We require a MPD to satisfy the unitary condition, i.e.,  $\hat{U}\hat{U}^\dagger = \hat{U}^\dagger\hat{U} = I$ . Then from Eq. (5), one can readily have  $|\psi\rangle = \hat{U}^\dagger|0\rangle$ , meaning  $\hat{U}^\dagger$  evolves the product state into the MPS.

In the following, we show how to define the MPD from a given MPS. The diagram of the MPD formed by eight tensors is illustrated in Fig. 1 (a) as an example. For the last tensor ( $N = 8$ ) of the MPD, we have

$$G^{[8]} = A^{[8]}, \quad (6)$$

which is just an one-qubit unitary gate [satisfying Eq. (3)].

For  $1 < n < N$ , the tensors in the MPD possess the dimension  $(d \times d \times d \times d)$ , which we denote as  $G_{ijkl}^{[n]}$ . Remind that for the moment, we assume  $d = \chi$  in the MPS (we will explain the reason later). The component of  $G^{[n]}$  by fixing  $i = 0$

is given by the corresponding tensor  $A^{[n]}$  in the MPS, i.e.,

$$G_{0jkl}^{[n]} = A_{jkl}^{[n]}. \quad (7)$$

The rest components for  $i = 1, \dots, d-1$  are obtained in the kernel subspace as the following. According to the orthogonal conditions of  $A^{[n]}$  [Eq. (3)], let us consider  $A_{jkl}^{[n]}$  with  $j = 0, \dots, d-1$  as orthonormal vectors in the  $d^2$ -dimensional vector space. Then choose  $(d^2 - d)$  orthonormal vectors in the kernel of  $A^{[n]}$  as  $G_{ij'kl}^{[n]}$  ( $i = 1, \dots, d-1$ ). These new components are orthogonal to the  $d$  vectors from  $A_{jkl}^{[n]}$ . Together with Eq. (7), we have

$$\sum_{kl} G_{i'j'kl}^{[n]} G_{ijkl}^{[n]*} = I_{i'i} I_{j'j}. \quad (8)$$

$G^{[n]}$  can always be defined in this way since  $\dim(i) \dim(j) = \dim(k) \dim(l) = d^2$ . Specifically for  $d = 2$ , one has  $\sum_{kl} G_{1j'kl}^{[n]} A_{jkl}^{[n]*} = 0$  and together  $\sum_{kl} G_{1j'kl}^{[n]} G_{1jkl}^{[n]*} = I_{j'j}$ . It means  $G_{10kl}^{[n]}$  and  $G_{11kl}^{[n]}$  are the two normalized vectors defined in the four-dimensional vector space that are orthogonal to  $G_{00kl}^{[n]}$  and  $G_{01kl}^{[n]}$ . These four vectors just form the complete orthonormal bases of this vector space. Eq. (8) gives the orthonormal conditions, and means that  $G^{[n]}$  is a two-qubit unitary gate.

For  $n = 1$ , the tensor is also forth-order, denoted as  $G_{ijkl}^{[1]}$ . The component by taking  $i = j = 0$  is given by  $A^{[1]}$ , i.e.,

$$G_{00kl}^{[1]} = A_{kl}^{[1]}. \quad (9)$$

$G_{00kl}^{[1]}$  is in fact a  $d^2$ -dimensional normalized vector [see Eq. (2)]. The rest  $(d^2 - 1)$  components of  $G_{ijkl}^{[1]}$  (with  $i \neq 0$  or  $j \neq 0$ ) are the orthonormal vectors in the kernel of  $A^{[1]}$ . The orthonormal conditions are the same as Eq. (8), which means that  $G^{[1]}$  is also a two-qubit gate. In short, the MPD  $\hat{U}$  of a given MPS  $|\psi\rangle$  can be obtained with Eqs. (6)-(9). Then by definition [Eqs. (6), (7), and (9)], we have  $|\psi\rangle = \hat{U}^\dagger|0\rangle$ .

We now prove that the MPD  $\hat{U}$  is unitary [Fig. 1 (b)], by using the orthonormal conditions [Eqs. (4) and (8)], illustrated at the top of Fig. 1 (b)]. First,  $G^{[8]}$  and  $G^{[8]*}$  vanish into an identity according to Eq. (4). Then, the rest of the gates result in the identities according to Eq. (8). Consequently, we have  $\hat{U}^\dagger\hat{U} = I$ . Since  $\hat{U}$  is in fact a  $(d^N \times d^N)$  square matrix, one readily has  $\hat{U}\hat{U}^\dagger = I$ .

In above, we have proven  $|\psi\rangle = \hat{U}^\dagger|0\rangle$  and  $\hat{U}^\dagger\hat{U} = \hat{U}\hat{U}^\dagger = I$ , from which we immediately have  $\hat{U}|\psi\rangle = |0\rangle$ . It means that  $\hat{U}$  exactly disentangles the MPS into a product state.

Since each tensor in the MPD is in fact a unitary gate, the MPD can be written as a quantum circuit, as shown in Fig. 1 (a). The correspondence of the indexes between the tensors of the MPD and the gates in the circuit are given at the bottom of the figure. Note the direction of the time flow in the quantum circuit is opposite to the direction that indicates the orthogonal conditions of the MPS. In the circuit, one acts from  $G^{[1]}$  to  $G^{[8]}$  on  $|0\rangle$ . From the diagram of the circuit, it requires

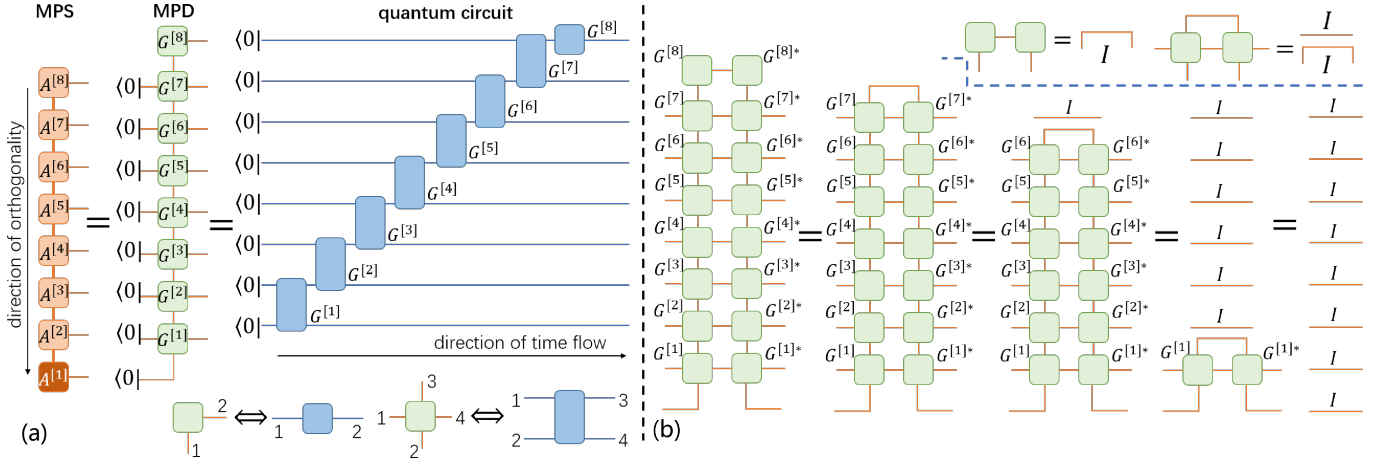


FIG. 1. (Color online) (a) The diagram of  $|\psi\rangle = \hat{U}^\dagger|0\rangle$ , where  $|\psi\rangle$  and  $\hat{U}$  represent the MPS and MPD, respectively. The diagram of the corresponding quantum circuit is also given. The correspondence of the indexes of the tensors in the MPD and the gates in the circuit is shown at the bottom. (b) The proof of  $\hat{U}\hat{U}^\dagger = I$ . The orthogonal conditions of the tensors in the MPD are given at the top.

$\dim(i) = \dim(k)$  and  $\dim(j) = \dim(l)$  since  $i$  and  $k$ ,  $j$  and  $l$  represent the same qubit, respectively. This means  $\chi = d$  in the MPS.

For the cases of  $\chi > d$ , the above method can still be used to define an MPD, which reduces the entanglement of the MPS. First, find the optimal MPS  $|\tilde{\psi}\rangle$  with  $\chi = d$  that maximizes the fidelity  $|\langle\psi|\tilde{\psi}\rangle|$ . This can be easily done by reducing the virtual bond dimensions of  $|\psi\rangle$  to  $d$  with the standard truncation algorithm of MPS (see a review of MPS [35] for example). Then, the MPD  $\hat{U}$  can be obtained from  $|\tilde{\psi}\rangle$  following the above procedure.  $\hat{U}$  cannot disentangle  $|\psi\rangle$  into a product state, but will largely reduce its entanglement.

We take the ground state of the 1D transverse Ising model as an example to testify the above scheme. The Hamiltonian is written as  $\hat{H} = \sum_{n=1}^{N-1} \hat{S}_n^z \hat{S}_{n+1}^z - h_x \sum_{n=1}^N \hat{S}_n^x$ . The MPS is obtained by DMRG algorithm [1, 2] with  $N = 48$  and  $\chi = 64 \gg d$  (note  $d = 2$  for the quantum Ising model). We calculate the negative-logarithmic fidelities (NLF) per site

$$F_0 = -\frac{\ln |\langle\psi|\tilde{\psi}_{\chi=1}\rangle|}{N}, \quad (10)$$

$$F_1 = -\frac{\ln |\langle\psi|\hat{U}^\dagger|0\rangle|}{N}. \quad (11)$$

In  $F_0$ , the state  $|\tilde{\psi}_{\chi=1}\rangle$  is an MPS with  $\chi = 1$  (a separable state) that is optimally truncated from  $|\psi\rangle$ .  $F_0$  is in fact the global distance between the MPS and a separable state [47].  $F_1$  characterizes the distance between  $|\psi\rangle$  and  $\hat{U}^\dagger|0\rangle$ , i.e., how accurately  $\hat{U}^\dagger$  evolves  $|0\rangle$  to the targeted MPS  $|\psi\rangle$ .

For  $h_x \ll h_c$  and  $h_x \gg h_c$  with  $h_c = 0.5$  the critical point (for  $N \rightarrow \infty$  strictly speaking, since criticality is defined in the thermodynamic limit),  $|\psi\rangle$  is in the Néel phase and polarized phase, respectively. The ground-state entanglement in these phases is small. However,  $F_0$  is still non-zero in these regions since the quantum fluctuations produce certain entanglement that requires  $\chi > 1$ . As expected, a peak of

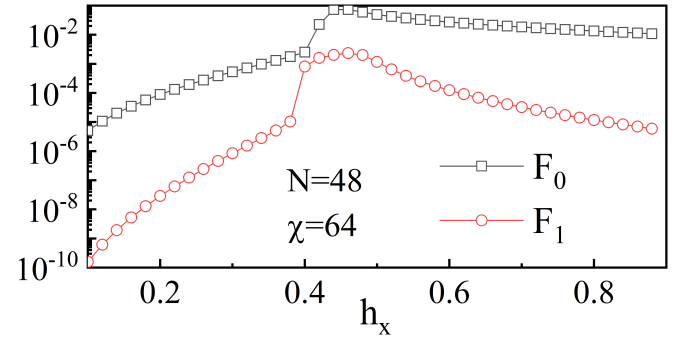


FIG. 2. (Color online) Semi-log plot of the NLF's  $F_0$  [Eq. (10)] and  $F_1$  [Eq. (11)] of the ground state of transverse Ising model with different magnetic field  $h_x$ .  $F_0$  characterizes the minimal distance between  $|\psi\rangle$  and a separable state.  $F_1$  characterizes how accurately the quantum circuit evolves the product state  $|0\rangle$  to the targeted MPS.

$F_0$  appears near the critical point, where  $|\psi\rangle$  is quite far away from a separable state.

After being acted by  $\hat{U}$ ,  $|\psi\rangle$  becomes much closer to the product state  $|0\rangle$ , as indicated by  $F_1$  that is about  $O(10) \sim O(10^4)$  smaller than  $F_0$ . In other words, the circuit  $\hat{U}^\dagger$ , which only contains one- and two-qubit gates, can accurately evolve  $|0\rangle$  to the targeted MPS with  $\chi \gg d$  and  $N \gg 1$ .

*Encoding matrix product state into deep quantum circuit.*— To further increase the accuracy, we propose an algorithm to encode a given MPS  $|\psi\rangle$  to a deep quantum circuit that contains multiple layers of MPD's [Fig. 3 (a)]. The depth of the circuit equals to the number of layers. The encoding algorithm is as following.

1. For the MPS  $|\psi_k\rangle$  in the  $k$ -th iteration (initialized as  $|\psi_0\rangle = |\psi\rangle$ ), compute the MPS  $|\tilde{\psi}_k\rangle$  of  $\chi = d$  by optimally truncating the virtual bond dimensions of  $|\psi_k\rangle$ ;
2. Compute the MPD  $\hat{U}_t$  with  $t = \mathcal{D} - k$ , which disent-

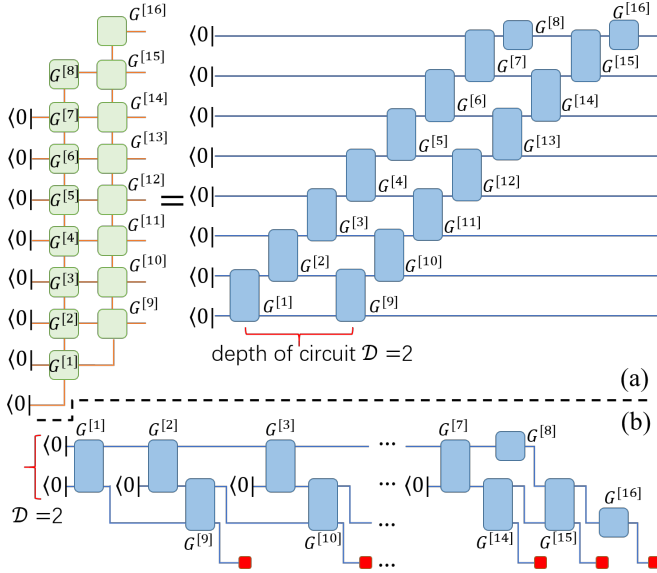


FIG. 3. (Color online) The diagrams of (a) the deep quantum circuit consisting of  $\mathcal{D} = 2$  layers of matrix product disentanglers, and (b) the qubit-efficient scheme of the circuit. In (b), we use the red squares to mark the degrees of freedom corresponding to the physical indexes of the MPS.

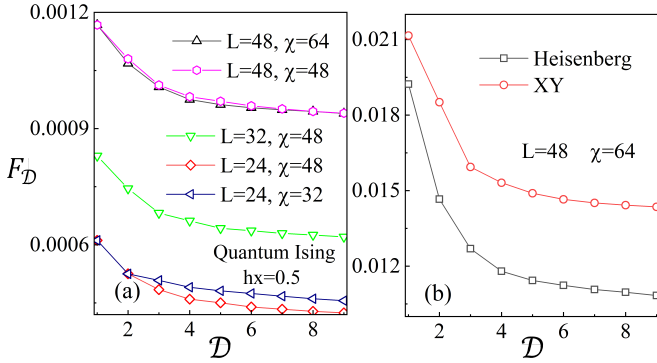


FIG. 4. (Color online) The NLF per site  $F_{\mathcal{D}}$  [Eq. 12] of the ground states of 1D (a) quantum Ising model at the critical point, and (b) Heisenberg and XY models, versus the depth of the quantum circuit  $\mathcal{D}$ .

gles  $|\tilde{\psi}_k\rangle$  to  $|0\rangle$ , using the method introduced in the last section;

3. Disentangle  $|\psi_k\rangle$  to  $|\psi_{k+1}\rangle$  as  $|\psi_{k+1}\rangle = \hat{U}_t |\psi_k\rangle$ .
4. Return the MPD's  $\{\hat{U}_t\}$  ( $t = 1, 2, \dots, \mathcal{D}$ ) when the required depth of the circuit is reached, or go back to Step 1 with  $|\psi_{k+1}\rangle$ .

We testify the encoding algorithm on the ground states of 1D transverse Ising, Heisenberg, and XY models. For the Heisenberg and XY models, the Hamiltonians are  $\hat{H} = \sum_n (\hat{S}_n^x \hat{S}_{n+1}^x + \hat{S}_n^y \hat{S}_{n+1}^y + \hat{S}_n^z \hat{S}_{n+1}^z)$  and  $\hat{H} = \sum_n (\hat{S}_n^x \hat{S}_{n+1}^x + \hat{S}_n^y \hat{S}_{n+1}^y)$ , respectively. These Hamiltonians are “nearly” gapless (as they are gapless in the thermodynamic limit), thus the

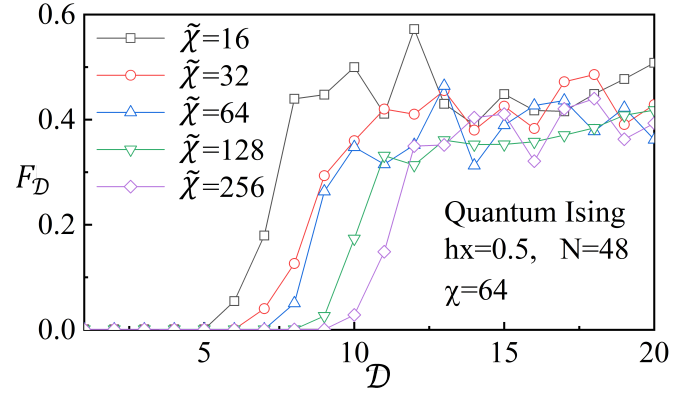


FIG. 5. (Color online) The NLF per site  $F_{\mathcal{D}}$  of the ground state of 1D quantum Ising model at the critical point versus the depth of the quantum circuit  $\mathcal{D}$ . Different dimension cut-offs  $\tilde{\chi}$  in the encoding algorithm are taken. The sudden increase of the NLF occurs at  $\mathcal{D} = \log_2 \tilde{\chi}$ .

MPS's of large  $\chi$ 's are required to approximately capture the entanglement. The NLF  $F_{\mathcal{D}}$  between the targeted state and the evolved state (Fig. 4) is defined as

$$F_{\mathcal{D}} = -\frac{\ln |\langle \psi | \hat{U}_{\mathcal{D}}^\dagger \cdots \hat{U}_2^\dagger \hat{U}_1^\dagger | 0 \rangle|}{N}. \quad (12)$$

One can see that the  $F_{\mathcal{D}}$  further decays with the depth of the circuit  $\mathcal{D}$ . Note that the largest drop of the NLF occurs for  $\mathcal{D} = 1$ , where  $F_{\mathcal{D}}$  is reduced by about  $O(10^2)$  times compared with  $F_0$ . For  $\mathcal{D} > 1$ , relatively large drops of  $F_{\mathcal{D}}$  occur for about  $\mathcal{D} \leq 4$ . With  $\mathcal{D} = 9$ , the NLF is reduced by about 20% ~ 40% compared with  $F_1$ .

The number for parameters is significantly compressed by encoding the MPS to the quantum circuit. With  $d = 2$  and  $\chi = 64$  as an example, the number (per site) for the original MPS  $\#(|\psi\rangle) = d\chi^2 = 2^{13}$  is significantly compressed to  $\#(\hat{U}) = \mathcal{D}d^4 = 2^7$  for  $\mathcal{D} = 8$ .

*Error propagations and complexity analyses.*— The computational cost of computing the MPD's by the encoding algorithm scales only linearly with  $\mathcal{D}$ , similar to the time-evolving block decimation algorithm [8, 11]. One can see that disentangling the state  $|\psi_{k+1}\rangle = \hat{U}_t |\psi_k\rangle$  in Step 3 will essentially increase exponentially the virtual dimensions of  $|\psi_k\rangle$  as  $\sim \chi d^k$ . Therefore, we set an upper bound of the virtual dimensions  $\tilde{\chi}$  and truncate if the dimensions exceed  $\tilde{\chi}$ . Same truncation rule is implemented when calculating  $F_{\mathcal{D}}$ . We find that such truncations will not affect the results too much if  $\mathcal{D} \leq \log_d \tilde{\chi}$ .

For  $\mathcal{D} > \log_d \tilde{\chi}$ , however, our data show that the error suddenly soars, and the results of fidelity become unreliable (Fig. 5). Such a “catastrophe” for  $\mathcal{D} > \log_d \tilde{\chi}$  is due to the propagations of the truncation errors: the errors in the encoding algorithm and those in the evolution by the circuit propagate in opposite directions.

In the encoding algorithm, the gates are computed in the order from  $\hat{U}_{\mathcal{D}}$  to  $\hat{U}_1$ . The error accumulates slowly in the same way. Differently for the circuit, the gates are acted to



$|0\rangle$  following the direction of time flow in the circuit (starting from  $\hat{U}_1^\dagger$  to  $\hat{U}_D^\dagger$ ). During the evolution, the virtual bond dimensions of  $|\phi_t\rangle = \hat{U}_t^\dagger \cdots \hat{U}_1^\dagger |0\rangle$  increases with  $t$  as  $\sim d^t$ . For  $D \leq \log_d \tilde{\chi}$ , there is no truncation error in  $|\phi_D\rangle$ , thus the error is robustly controlled by the truncation errors in the encoding algorithm, and  $F_D$  decays with  $D$  as expected. For  $D > \log_d \tilde{\chi}$ , truncations have to be implemented for the evolutions of  $D \geq t > \log_d \tilde{\chi}$ . These truncations actually occur at small  $k$ 's in the encoding scheme, thus will raise the error as soon as the truncations on  $|\phi_t\rangle$  are implemented. This makes the computational complexity exponentially high, since one needs to keep exponentially large  $\tilde{\chi} \sim d^D$  to avoid the ‘‘catastrophe’’.

Considering the complexity of the quantum circuit, the numbers of both the gates and qubits in our quantum circuit scale linearly with  $N$  and  $D$  [Fig. 3 (a)]. By incorporating with the efficient-qubit scheme [27], the number of needed qubits is compressed to be independent on  $N$  and to scale only with  $D$  linearly [Fig. 3 (b)]. This largely reduces the difficulty of realizing our circuit on the near-term quantum platforms.

**Summary.**— Encoding an  $N$ -qubit MPS with large virtual dimensions to a quantum circuit is an important but extremely challenging task. In this work, we propose an efficient and accurate algorithm that encodes a given MPS into a quantum circuit that consists of only one- and two-qubit gates. We testified our algorithm on several MPS's that describe the ground states of the ‘‘nearly’’ gapless Hamiltonians. These MPS's possess large entanglement, thus are difficult to encode using the existing methods. Our data show that with less than 10 qubits, the quantum circuit constructed by our algorithm can accurately evolve a product state to the targeted MPS which might even have large virtual dimensions and/or system size.

**Acknowledgment.**— SJR is grateful to Jin-Guo Liu for stimulating discussions and useful information. This work was supported by Beijing Natural Science Foundation (Grant No. 1192005 and No. Z180013) and the NSFC (Grant No. 11834014).

---

\* Email: [sjran@cnu.edu.cn](mailto:sjran@cnu.edu.cn)

- [1] S. R. White, *Phys. Rev. Lett.* **69**, 2863 (1992).
- [2] S. R. White, *Phys. Rev. B* **48**, 10345 (1993).
- [3] S. Moukouri and L. G. Caron, *Phys. Rev. Lett.* **77**, 4640 (1996).
- [4] X. Wang and T. Xiang, *Phys. Rev. B* **56**, 5061 (1997).
- [5] E. Bartel, A. Schadschneider, and J. Zittartz, *J. Eur. Phys. J. B* **31**, 209 (2003).
- [6] S. G. Chung and L. Wang, *Phys. Lett. A* **373**, 2277 (2009).
- [7] J. Haegeman, B. Pirvu, D. J. Weir, J. I. Cirac, T. J. Osborne, H. Verschelde, and F. Verstraete, *Phys. Rev. B* **85**, 100408 (2012).
- [8] G. Vidal, *Phys. Rev. Lett.* **93**, 040502 (2004).
- [9] F. Verstraete, J. J. Garcia-Ripoll, and J. I. Cirac, *Phys. Rev. Lett.* **93**, 207204 (2004).
- [10] F. Verstraete and J. I. Cirac, *Phys. Rev. B* **73**, 094423 (2006).
- [11] G. Vidal, *Phys. Rev. Lett.* **98**, 070201 (2007).
- [12] W. Li, S.-J. Ran, S.-S. Gong, Y. Zhao, B. Xi, F. Ye, and G. Su, *Phys. Rev. Lett.* **106**, 127202 (2011).
- [13] T. H. Johnson, S. R. Clark, and D. Jaksch, *Phys. Rev. E* **82**, 036702 (2010).
- [14] T. Prosen and M. Žnidarič, *J. Stat. Mech.* **2009**, P02035 (2009).
- [15] F. A. Wolf, I. P. McCulloch, and U. Schollwöck, *Phys. Rev. B* **90**, 235131 (2014).
- [16] F. A. Y. N. Schröder and A. W. Chin, *Phys. Rev. B* **93**, 075105 (2016).
- [17] D. Jaschke, S. Montangero, and L. D. Carr, *Quantum Sci. Technol.* **4**, 013001 (2018).
- [18] J. I. Cirac and G. Sierra, *Phys. Rev. B* **81**, 104431 (2010).
- [19] F. Verstraete and J. I. Cirac, *Phys. Rev. Lett.* **104**, 190405 (2010).
- [20] J. Haegeman, J. I. Cirac, T. J. Osborne, and F. Verstraete, *Phys. Rev. B* **88**, 085118 (2013).
- [21] A. Milsted, J. Haegeman, and T. J. Osborne, *Phys. Rev. D* **88**, 085030 (2013).
- [22] A. Steffens, C. A. Riofrío, R. Hübener, and J. Eisert, *New J. Phys.* **16**, 123010 (2014).
- [23] J. Rincón, M. Ganahl, and G. Vidal, *Phys. Rev. B* **92**, 115107 (2015).
- [24] E. Stoudenmire and D. J. Schwab, in *Advances in Neural Information Processing Systems 29*, edited by D. D. Lee, M. Sugiyama, U. V. Luxburg, I. Guyon, and R. Garnett (Curran Associates, Inc., 2016) pp. 4799–4807.
- [25] Z.-Y. Han, J. Wang, H. Fan, L. Wang, and P. Zhang, *Phys. Rev. X* **8**, 031012 (2018).
- [26] J. Chen, S. Cheng, H. Xie, L. Wang, and T. Xiang, *Phys. Rev. B* **97**, 085104 (2018).
- [27] W. Huggins, P. Patil, B. Mitchell, K. B. Whaley, and E. M. Stoudenmire, *Quantum Sci. Technol.* **4**, 024001 (2019).
- [28] Z.-Z. Sun, C. Peng, D. Liu, S.-J. Ran, and G. Su, (2019), [arXiv:1903.10742](https://arxiv.org/abs/1903.10742).
- [29] F. Verstraete, D. Porras, and J. I. Cirac, *Phys. Rev. Lett.* **93**, 227205 (2004).
- [30] D. Gross, J. Eisert, N. Schuch, and D. Perez-Garcia, *Phys. Rev. A* **76**, 052315 (2007).
- [31] F. Verstraete, M. M. Wolf, and J. I. Cirac, *Nat. phys.* **5**, 633 (2009).
- [32] A. Dang, C. D. Hill, and L. C. Hollenberg, *Quantum* **3** (2019), 10.22331/q-2019-01-25-116.
- [33] A. S. Bhatia and M. K. Saggi, (2018), [arXiv:1811.09833](https://arxiv.org/abs/1811.09833).
- [34] I. Affleck, T. Kennedy, E. H. Lieb, and H. Tasaki, *Phys. Rev. Lett.* **59**, 799 (1987).
- [35] D. Pérez-García, F. Verstraete, M. M. Wolf, and J. I. Cirac, *Quantum Inf. Comput.* **7**, 401 (2007).
- [36] T.-C. Wei, I. Affleck, and R. Raussendorf, *Phys. Rev. Lett.* **106**, 070501 (2011).
- [37] D. V. Else, I. Schwarz, S. D. Bartlett, and A. C. Doherty, *Phys. Rev. Lett.* **108**, 240505 (2012).
- [38] C. Song, K. Xu, H. Li, Y.-R. Zhang, X. Zhang, W. Liu, Q. Guo, Z. Wang, W. Ren, J. Hao, *et al.*, *Science* **365**, 574 (2019).
- [39] A. Barenco, C. H. Bennett, R. Cleve, D. P. DiVincenzo, N. Margolus, P. Shor, T. Sleator, J. A. Smolin, and H. Weinfurter, *Phys. Rev. A* **52**, 3457 (1995).
- [40] F. T. Chong, D. Franklin, and M. Martonosi, *Nature* **549**, 180 (2017).
- [41] J.-G. Liu, Y.-H. Zhang, Y. Wan, and L. Wang, (2019), [arXiv:1902.02663](https://arxiv.org/abs/1902.02663).
- [42] M. Mottonen and J. J. Vartiainen, ‘‘Decompositions of general quantum gates,’’ in *Trends in Quantum Computing Research*, edited by S. Shannon (NOVA Publishers, New York, 2006) p. Chapter 7.
- [43] J. I. Cirac, D. Perez-Garcia, N. Schuch, and F. Verstraete, *J.*

- [Stat. Mech.](#) **2017**, 083105 (2017).
- [44] G. Vidal, J. I. Latorre, E. Rico, and A. Kitaev, [Phys. Rev. Lett.](#) **90**, 227902 (2003).
- [45] L. Tagliacozzo, T. de Oliveira, S. Iblisdir, and J. I. Latorre, [Phys. Rev. B](#) **78**, 024410 (2008).
- [46] U. Schollwöck, [Ann. Phys.](#) **326**, 96 (2011).
- [47] T.-C. Wei and P. M. Goldbart, [Phys. Rev. A](#) **68**, 042307 (2003).